Comparison of Constraint-handling Methods for the Sequential Approximate Optimization of Functionally Graded Plates

Leonardo G. Ribeiro[1], Evandro Parente Jr.[1], Antônio M. C. de Melo[1]

[1]*Departamento de Engenharia Estrutural e Construção Civil, Universidade Federal do Ceará*
Campus do Pici, Bloco 728, 60440-900, Ceará-Brazil
leonardoribeiro@alu.ufc.br, evandro@ufc.br, macario@ufc.br

Abstract. The optimal material design in Functionally Graded (FG) structures can be defined by an optimization procedure. This is often performed by the use of bio-inspired algorithms, even though they may require thousands of function evaluations. Alternatively, a surrogate model can be used to provide a faster assessment of the structural response. In this work, the Sequential Approximate Optimization (SAO) will be employed, where the approximate surface will be iteratively improved by the addition of new points in regions of interest. When constraint functions need to be approximated by a surrogate model, a feasibility function can be considered to account for the uncertainty in determining the design's feasibility. The SAO approach will be employed in the optimization of Functionally Graded Plates considering expensive constraints, and different feasibility functions will be tried out. The optimization will also be carried out using a bio-inspired algorithm, and these approaches will be compared in terms of efficiency and accuracy.

Keywords: Sequential Approximate Optimization, Constraint-handling methods, Functionally Graded Materials, Kriging.

1 Introduction

Functionally Graded Materials (FGMs) are a class of smart composite materials where, given a set gradation between two or more materials, equivalent material properties smoothly change over a given direction [1]. This feature allows for an efficient use of each constituent, while also avoiding disadvantages often seen in laminated structures such as delamination and stress concentrations [2].

To define the optimal material gradation, one may employ an optimization procedure. In structural optimization problems, it is usual to use bio-inspired algorithms, such as the Particle Swarm Optimization (PSO) [2]. However, bio-inspired methods often need to perform hundreds or even thousands of function evaluations, which can become very costly when numerical methods are employed, e.g. Finite Element Method (FEM) or Isogeometric Analysis (IGA).

To deal with this issue, costly functions may be approximated by a surrogate model (e.g. Kriging [3]). In this study, we will make use of the Sequential Approximate Optimization (SAO), which aims at iteratively improving the model by the addition of new sampling points in regions of interest. These regions may be defined by the use of an acquisition function, such as the Expected Improvement (EI) [4]. The acquisition function should consider both the exploitation and the exploration of the design space. For constrained problems, the choice of new points should also consider the constraints in some way.

For expensive constraint functions, these should also be approximated by a surrogate model. However, due to model uncertainty, it is not easy to determine the feasibility of a given design based on the approximation itself [5]. Different researchers proposed feasibility functions which penalize unfeasible designs, taking model uncertainty in consideration [5–7]. However, to this day, there is no silver bullet to handle constrained optimization in SAO [8].

This study aims at performing a comparison between different constraint-handling methods for the Sequential Approximate Optimization of Functionally Graded Plates (FGP) with respect to accuracy and computational efficiency. These are also compared to the optimization of FGP using bio-inspired algorithms, and the results for

the Particle Swarm Optimization (PSO) are presented.

This paper is organized as follows. In Section 2 the Functionally Graded Plates (FGP) are described in more detail. In Section 3 the operators and parameters of the PSO are introduced. In Section 4 the SAO approach is explained, and the Kriging model building and constrained infill criteria are discussed. The results are presented in Section 5, and the main conclusions are brought together in Section 6.

2 Functionally Graded Plates

This paper will deal with Functionally Graded Plates made of two materials, a ceramic c and a metal m, where the material gradation varies through the structure thickness. Usually, the volume fraction variation is controlled by different one-parameter functions, such as power-law and sigmoid functions [9]. To enhance design flexibility, B-Splines are also employed to define the material gradation [10]:

$$V_c(\xi) = \sum_{i=1}^{n_{cp}} B_{i,p}(\xi)\, V_{c,i}, \quad V_m(\xi) = 1 - V_c(\xi) \quad \xi \,\epsilon\, [0,1] \tag{1}$$

where n_{cp} is the number of control points, $V_{c,i}$ is the fraction of the ceramic volume of the i-th control point, $B_{i,p}(\xi)$ is the corresponding B-Spline base, p is the base degree and ξ is the parametric coordinate. The B-Spline base is evaluated by the Cox-de Boor formula, given a node vector $\Xi = [\xi_1, \xi_2, ..., \xi_{n+p+1}]$ [11].

The assessment of the effective properties at a given point of the structure are performed by the Mori-Tanaka scheme [1], where the structure, formed by a material m, is assumed to be reinforced by spherical particles from material c. Thus, the mechanical properties can be evaluated by:

$$\frac{K(z) - K_m}{K_c - K_m} = \frac{V_c(z)}{1 + \dfrac{3\,V_m(z)\,(K_c - K_m)}{3\,K_m + 4\,G_m}}, \quad \frac{G(z) - G_m}{G_c - G_m} = \frac{V_c(z)}{1 + \dfrac{V_m(z)\,(G_c - G_m)}{G_m + f_m}} \tag{2}$$

where:

$$f_m = \frac{G_m\,(9\,K_m + 8\,G_m)}{G_m + f_m} \tag{3}$$

Then, the Young's modulus (E) and Poisson's ratio (ν) are computed according to standard expressions [1].

3 Particle Swarm Optimization

The Particle Swarm Optimization (PSO) was first proposed by Kennedy and Eberhart [12]. Soon, different versions were proposed, where researchers would suggest improvements to the initial formulation [13]. In this work, the version presented in Barroso et al. [14] is employed.

The PSO is initialized by generating N_p random particles. Each particle j is assigned a position $\mathbf{x}_j^0$ and a velocity $\mathbf{v}_j^0$. At each iteration, the particles move in the design space according to their velocity:

$$\mathbf{x}_j^{i+1} = \mathbf{x}_j^i + \mathbf{v}_j^{i+1}, \text{ where } \mathbf{v}_j^{i+1} = w\,\mathbf{v}_j^i + c_1\,r_1\,(\mathbf{x}_{p,j}^i - \mathbf{x}_j^i) + c_2\,r_2\,(\mathbf{x}_{g,j}^i - \mathbf{x}_j^i) \tag{4}$$

where w is the inertia, c_1 is the cognitive factor, c_2 is the social factor, $\mathbf{x}_{p,j}^i$ is the best position the particle j obtained during the optimization, and $\mathbf{x}_{g,j}^i$ is the best position the particles on the neighborhood of particle j obtained during the optimization. The parameters r_1 and r_2 are uniformly distributed random numbers between 0 and 1.

The definition of $\mathbf{x}_{g,j}^i$ depends on the Swarm topology. In this work, the Global topology is employed, where all particles are connected. Thus, $\mathbf{x}_{g,j}^i$ is the best position found among all particles. To improve the exploration in the design space, Barroso et al. [14] proposes the consideration of a mutation operator, where each variable has a small probability (p_{mut}) of mutating to a new random value inside the design space.

During the optimization process, a particle may violate a bound constraint leaving the design space. To avoid this from happening, when a particle leaves the search space, the variable that had its bounds violated is set to the bound, and its velocity is modified to the opposite direction [14]. On the other hand, implicit constraints can be handled by a exterior penalty approach, such as the static [10] or the adaptive [15] penalties.

The PSO algorithm is carried out until a stopping criteria is met, usually related to a maximum number of iterations It_{max} or a maximum number of consecutive iterations with no considerable improvement It_{stall}.

4 Sequential Approximate Optimization

While bio-inspired algorithms are very effective in finding the optimum for structural problems, they often require the evaluation of hundreds or even thousands of design points [10]. To improve computational efficiency, this study will employ the Sequential Approximate Optimization.

In SAO, an expensive function is replaced by an approximate response surface based on a small set of sampling points. In this work, this response surface is given by the Kriging model [3]. Then, new sampling points will be iteratively added in regions of interest, so that the model accuracy is improved [4]. The new points are chosen by a given infill criterion.

At the start of the algorithm, since no information about the function behavior is known, a Design of Experiments (DoE) technique can be employed to pick the initial sampling points. This work will use the Latin Hypercube Sampling (LHS), a stratified random sampling technique commonly employed for Surrogate-Based Optimization. To obtain a good initial sample, 20 different LHS samples will be generated, and the one where the minimum distance between two points is maximized is selected to perform the model building [10].

The following sections further describe the building process of the Kriging model and the infill criteria considered, including the handling of approximate constraint functions.

4.1 Kriging

In its general form, the Kriging model [3] can be given by the sum of a global trend (g) and its autocorrelated localized deviations (Z):

$$\hat{y}(\mathbf{x}) = g(\mathbf{x}) + Z(\mathbf{x}) \tag{5}$$

where $Z(\mathbf{x})$ can be assumed as the realization of a stochastic process with mean zero and covariance given by:

$$\text{cov}(\mathbf{y}, \mathbf{y}) = \sigma^2 \, \mathbf{\Psi} \tag{6}$$

where σ^2 is the process variance and $\mathbf{\Psi}$ is a correlation matrix.

We may define the correlation between the responses by the Gaussian kernel:

$$\text{cor}\left[y(\mathbf{x}_i), y(\mathbf{x}_j)\right] = \exp\left(-\sum_{k=1}^{m} \theta_k \left|x_{i,k} - x_{j,k}\right|^{p_k}\right) \tag{7}$$

which allows us to define a correlation matrix as:

$$\Psi_{ij} = \text{cor}[y(\mathbf{x}_i), y(\mathbf{x}_j)] \tag{8}$$

The computation of $\mathbf{\Psi}$ requires the definition of the hyper-parameters θ_k and p_k. These can be defined using the Maximum Likelihood Estimator (MLE). For a given data set $\mathcal{D} = \{(\mathbf{x}_i, y_i)\}_{i=1}^{n}$, the likelihood of a model with mean μ and variance σ is given by:

$$L(\mathbf{y}|\mu, \sigma) = \frac{1}{(2\,\pi\,\sigma^2)^{n/2}\,|\mathbf{\Psi}|^{1/2}} \, \exp\left[-\frac{(\mathbf{y} - \mathbf{1}\,\mu)^T \, \mathbf{\Psi}^{-1} \, (\mathbf{y} - \mathbf{1}\,\mu)}{2\,\sigma^2}\right] \tag{9}$$

By differentiation, we obtain the MLE for μ and σ as:

$$\hat{\mu} = \frac{\mathbf{1}^T \mathbf{\Psi}^{-1} \mathbf{y}}{\mathbf{1}^T \mathbf{\Psi}^{-1} \mathbf{1}} \quad \hat{\sigma}^2 = \frac{(\mathbf{y} - \mathbf{1}\hat{\mu})^T \mathbf{\Psi}^{-1} (\mathbf{y} - \mathbf{1}\hat{\mu})}{n} \tag{10}$$

However, we are not able to define θ_k or p_k in the same way. Instead, we need to use an optimization method to define the optimum value for these parameters. For simplification purposes, in this work we consider $p_k = 2.0$, and perform the optimization solely over the parameter θ_k [3]. Substituting Eq. (10) in Eq. (9), taking the natural logarithm and removing the constant terms, we end up with the concentrated ln-likelihood function:

$$\ln L \approx -\frac{n}{2} \, \ln(\hat{\sigma}^2) - \frac{1}{2} \, \ln|\mathbf{\Psi}| \tag{11}$$

Thus, the definition of θ_k may be performed by solving the following optimization problem:

$$\begin{cases} \text{minimize} & -\ln L(\boldsymbol{\theta}) \\ \text{where} & \boldsymbol{\theta}_L \leq \boldsymbol{\theta} \leq \boldsymbol{\theta}_U \end{cases} \tag{12}$$

Since the evaluation of the objective function is usually not costly, we may perform this procedure using a bio-inspired optimization algorithm, such as the Particle Swarm Optimization.

After the model is built, we can assess the model prediction using the Kriging estimator, given by [3]:

$$\hat{y}(\mathbf{x}) = \hat{\mu} + \boldsymbol{\psi}^T \, \mathbf{\Psi}^{-1} \, (\mathbf{y} - \mathbf{1}\,\hat{\mu}) \tag{13}$$

4.2 Infill criteria

After the model is built, it can be used to guide the further selection of new points in regions of interest. Ideally, the infill criterion should consider the model uncertainty in regions far from the sampling points. Due to the theory behind Gaussian Processes (GPs), we may evaluate the Kriging model posterior variance by [3]:

$$\hat{s}^2(\mathbf{x}) = \sigma^2 \left(1 - \boldsymbol{\psi}^T \boldsymbol{\Psi}^{-1} \boldsymbol{\psi}\right) \tag{14}$$

which can be understood as an estimate of how certain the model is about its own prediction. Figure 1 shows the confidence interval ($\hat{y} \pm \hat{s}$) for the Kriging prediction for a given one-dimensional function. Note that the variance is zero at the sampling points, but it increases as x gets farther from them.

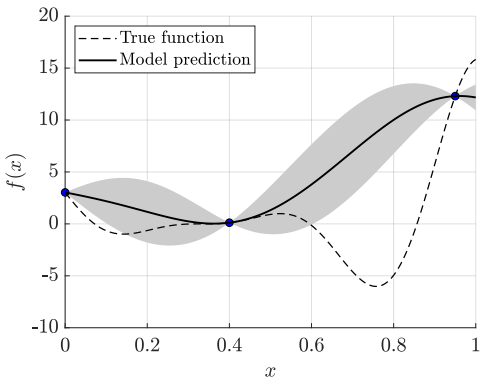

Figure 1. Kriging confidence interval for a one-dimensional function.

The infill criterion is often given by the optimization of a given acquisition function, which can be based both on the model prediction $\hat{y}(\mathbf{x})$ and variance $\hat{s}(\mathbf{x})$. For example, on the Efficient Global Optimization (EGO) algorithm, the model is iteratively improved by the addition of the point which maximizes the Expected Improvement (EI), given by:

$$E[I(\mathbf{x})] = (y_{min} - \hat{y}(\mathbf{x}))\, \Phi\left(\frac{y_{min} - \hat{y}(\mathbf{x})}{\hat{s}(\mathbf{x})}\right) + \hat{s}(\mathbf{x})\, \phi\left(\frac{y_{min} - \hat{y}(\mathbf{x})}{\hat{s}(\mathbf{x})}\right) \tag{15}$$

where Φ is the Cumulative Distribution Function (CDF) and ϕ is the Probability Density Function (PDF), both for the Normal distribution. This criterion is able to balance the exploitation (related to the first term) and the exploration (related to the second term). For constrained optimization, the constraint function should be taken into account, as only feasible individuals can improve upon the optimum. A feasibility function $F_j(\mathbf{x})$ based on the constraint function can be considered penalizing the EI by:

$$CE[I(\mathbf{x})] = \prod F_j(\mathbf{x})\, E[I(\mathbf{x})] \tag{16}$$

If constraint functions are cheap to evaluate, the feasibility function can be given by a simple step function as:

$$\mathrm{F}_j(\mathbf{x}) = \begin{cases} 0 & \text{, if } g_j(\mathbf{x}) > 0 \\ 1 & \text{, otherwise} \end{cases} \tag{17}$$

For expensive constraint functions, these should be approximated by a surrogate model $\hat{g}_j(\mathbf{x})$. In a similar manner, a direct approach is to simply consider that, if $\hat{g}_j(\mathbf{x}) > 0$, the EI is set to zero [16]. However, for approximate constraint functions, it might be wise to consider the model uncertainty in some way for Surrogate-Based Optimization (SBO). Schonlau et al. [5] proposed the use of the Probability of Feasibility (PF), where:

$$F(\mathbf{x}) = \Phi[\overline{g}_j(\mathbf{x})] = \frac{1}{2} + \frac{1}{2}\,\mathrm{erf}\left[\overline{g}_j(\mathbf{x})\right], \text{ where } \overline{g}_j(\mathbf{x}) = -\frac{\hat{g}_j(\mathbf{x})}{\hat{s}_j(\mathbf{x})} \tag{18}$$

Recently, Tutum et al. [6] and Bagheri et al. [7] also proposed different feasibility functions, denominated here as FFT and FFB, respectively. These change how the uncertainty is considered:

$$\mathrm{FFT}_j(\mathbf{x}) = \begin{cases} 2 - \mathrm{erf}\left(\overline{g}_j(\mathbf{x})\right) & \text{, if } 0 < \mathrm{erf}\left(\overline{g}_j(\mathbf{x})\right) \leq 1 \\ 0 & \text{, otherwise} \end{cases} \qquad \mathrm{FFB}_j(\mathbf{x}) = \min\left(2\,\Phi\left(\overline{g}_j(\mathbf{x})\right), 1\right) \tag{19}$$

Figure 2 shows how $F(\mathbf{x})$ behaves for these different approaches. In this work, these will be compared in the constrained optimization of FGP. It should be noted that, for cases where only the constraints are expensive to evaluate, the EI can be replaced by the actual improvement [17]:

$$I(\mathbf{x}) = \max(y_{min} - y(\mathbf{x}), 0), \text{ and } CI(\mathbf{x}) = \prod F_j(\mathbf{x})\, I(\mathbf{x}) \tag{20}$$

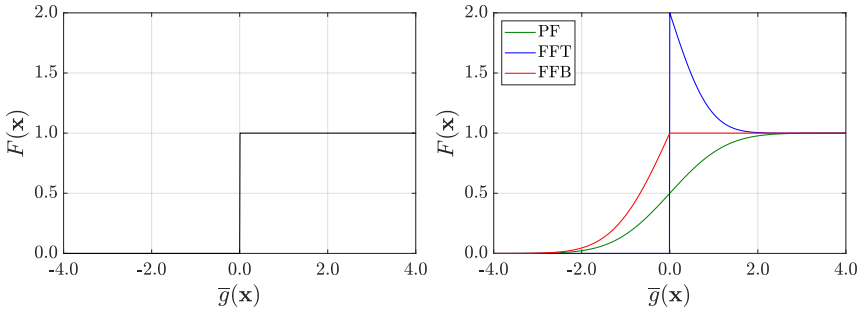

(a) Direct approach (b) Other methods

Figure 2. Different feasibility functions.

5 Numerical example

In this section, the mass minimization of a circular plate of Al/Al_2O_3 will be performed. Two constraints will be considered, related to the plate fundamental frequency and to the ceramic volume fraction. The material gradation is defined by a symmetric B-Spline with 9 control points, and the design variables are the plate thickness and the volume fraction for each control point. Due to symmetry, there are only six design variables. The optimization problem may be stated as:

$$\begin{cases} \text{minimize} & \pi\, R^2 \int_{-h/2}^{h/2} \rho(z)\ dz \\ \text{subjected to} & g_1(\mathbf{x}) = \omega(\mathbf{x}) - \omega_{max} \leq 0 \quad \text{and} \quad g_2(\mathbf{x}) = \dfrac{1}{h} \int_{-h/2}^{h/2} V_c\, dz - \overline{V}_{c,max} \leq 0 \\ \text{where} & h_{min} \leq x_1 \leq h_{max} \leq 0 \quad \text{and} \quad 0 \leq x_i \leq 1 \quad \text{for } i = 2, 3, \ldots 6 \end{cases} \tag{21}$$

where the maximum fundamental frequency is $\omega_{max} = 1000$ Hz and the maximum ceramic volume fraction is $\overline{V}_{c,max} = 35\%$. Table 1 presents the properties of each constituent, and effective properties are defined via the Mori-Tanaka model. Isogeometric Analysis is performed using a 256-element NURBS mesh, shown in Figure 3, along with the optimum design for this problem.

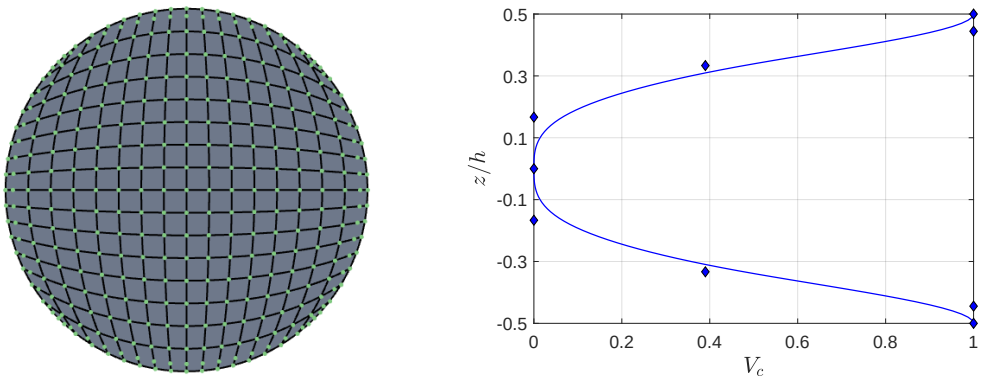

(a) NURBS mesh employed. (b) Optimum design distribution.

Figure 3. Circular plate optimization problem.

Results will be compared in terms of the average Normalized Root Mean Squared Error (NRMSE), the total number of evaluations n_{ev}, and the average Wall-Clock Time (WCT) spent for each optimization. In all cases, 10

Table 1. Material properties.

Material	E (GPa)	ν	ρ (kg/m^3)
Al	70	0.3000	2707
Al_2O_3	380	0.3262	3800

optimizations will be performed. All numerical computations were performed on a computer with a core i7-5500U CPU of 2.40 GHz clock speed and 16 GB of RAM. No parallelization procedure was used.

The problem was first solved using the PSO algorithm, considering a population $N_p = 50$ particles, and the stopping criteria are given by $It_{max} = 150$ and $It_{stall} = 20$. The optimum is found for $\mathbf{x} = [0.0197, 1.00, 1.00, 0.39, 0.00, 0.00]$, which presented a mass of 47.87 kg. Both constraints are active for the optimum design.

Then, the Sequential Approximate Optimization was performed. The initial model was built using 30 initial sampling points. The maximum number of sampling points is 100, but the algorithm may also stop earlier after a maximum number of consecutive iterations with no improvement $It_{stall} = 20$. The approximate response surface was created using a Kriging model. In this problem, only the assessment of the fundamental frequency is expensive. Thus, the model is built only for the constraint function related to the fundamental frequency.

Table 2 shows the results found for the feasibility functions tried out in this paper. Here, SAO algorithms are also compared to the PSO. The PSO presents a lower error when an adaptive penalty is employed. However, the bio-inspired algorithm requires thousands of high-fidelity evaluations, which results in a very high Wall-Clock Time. Meanwhile, the SAO algorithms requires, in all cases, less than 60 evaluations. This allows for a gain in efficiency, where SAO algorithms are almost 10 times faster than the PSO in terms of the WCT.

Table 2. Results found for the mass minimization of the circular FGP

Algorithm	NRMSE	n_{ev}	WCT (s)
SAO-Direct	2.58%	52	511
SAO-PF	0.59%	57	653
SAO-FFT	4.00%	50	473
SAO-FFB	0.47%	58	676
PSO-Static	0.13%	4630	6544
PSO-Adaptive	0.08%	5545	7834

In terms of the NRMSE, the best performing constraint-handling approaches were the Probability of Feasibility (PF) and the feasibility function proposed by Bagheri et al. [7], denominated here as FFB. These presented the lowest NRMSE, comparable to the one presented by the PSO. On the other hand, the feasibility function proposed by Tutum et al. [6] presented a NRMSE higher than the direct approach.

Finally, Figure 4 presents the boxplots of the NRMSE. The FFT approach is clearly the worst one, as some cases presented an NRMSE $> 10\%$. Taking a closer look to the PF and the FFB, we can see that, in some cases, these approaches are able to find designs even better than the those found by the PSO.

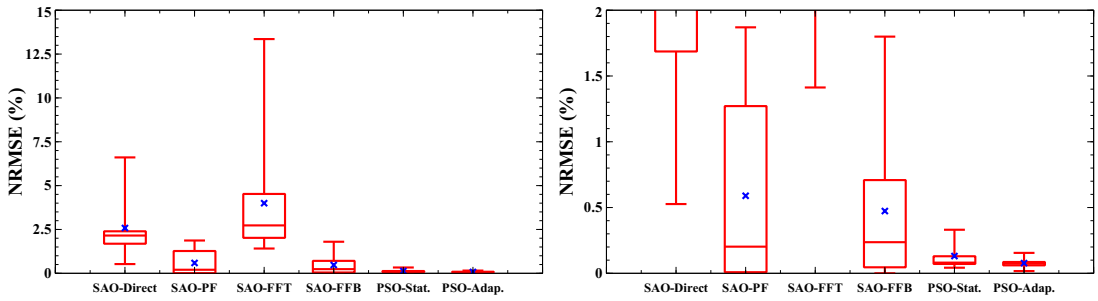

(a) All approaches.

(b) Closer look to the best-performing methods.

Figure 4. NRMSE boxplots for the mass minimization problem.

6 Conclusion

In this paper, the Sequential Approximate Optimization of a Functionally Graded Plate was performed, based on a Kriging surrogate. A comparison between different constraint-handling methods was presented, to understand which is able to provide the best results for cases where the constraint functions are expensive to evaluate, which is common in engineering design. All results were compared to the PSO, a bio-inspired algorithm commonly employed in the optimization of FGP, in terms of accuracy and efficiency.

It was shown that the SAO can provide a major gain in efficiency for the optimization when numerical analysis methods are employed, speeding up the process about 10 times. However, some constraint-handling approaches were not able to provide good results, on average. The best approaches were found to be the Probability of Feasibility (PF), proposed by Schonlau et al. [5], and the feasibility function proposed by Bagheri et al. [7]. These presented a low NRMSE, comparable to the PSO, and, in some cases, these were able to find designs even better than the best design found by the conventional bio-inspired method.

Acknowledgements. The financial support by CNPq (Conselho Nacional de Desenvolvimento Científico e Tecnológico) is gratefully acknowledged.

Authorship statement. The authors hereby confirm that they are the sole liable persons responsible for the authorship of this work, and that all material that has been herein included as part of the present paper is either the property (and authorship) of the authors, or has the permission of the owners to be included here.

References

[1] H. S. Shen. *Functionally graded materials: Nonlinear analysis of plates and shells*. CRC Press, 2009.
[2] S. Nikbakt, S. Kamarian, and M. Shakeri. A review on optimization of composite structures Part I: Laminated Composites. *Composite Structures*, vol. 195, pp. 158–185, 2018.
[3] A. I. J. Forrester, A. Sobester, and A. J. Keane. *Engineering design via surrogate modelling: a practical guide*. Wiley, 2008.
[4] D. R. Jones, M. Schonlau, and W. J. Welch. Efficient global optimization of expensive black-box functions. *Journal of Global Optimization*, vol. 13, pp. 455–492, 1998.
[5] M. Schonlau, W. J. Welch, and D. R. Jones. Global versus local search in constrained optimization of computer models. *New developments and applications in experimental design*, vol. Volume 34, pp. 11–25, 1998.
[6] C. C. Tutum, K. Deb, and I. Baran. Constrained efficient global optimization for pultrusion process. *Materials and Manufacturing Processes*, vol. 30, n. 4, pp. 538–551, 2014.
[7] S. Bagheri, W. Konen, R. Allmendinger, J. Branke, K. Deb, J. Fieldsend, D. Quagliarella, and K. Sindhya. Constraint handling in efficient global optimization. *Proceedings of the Genetic and Evolutionary Computation Conference*, vol. 17, pp. 673–680, 2017.
[8] J. Stork, M. Friese, M. Zaefferer, T. Bartz-beielstein, A. Fischbach, B. Breiderhoff, B. Naujoks, and T. Tusar. *Open Issues in Surrogate-Assisted Optimization*. Springer International Publishing, 2020.
[9] S. Nikbakht, S. Kamarian, and M. Shakeri. A review on optimization of composite structures part ii: Functionally Graded Materials. *Composite Structures*, vol. 214, pp. 83–102, 2019.
[10] L. G. Ribeiro, M. A. Maia, E. Parente Jr.., and A. M. C. D. Melo. Surrogate based optimization of functionally graded plates using radial basis functions. *Composite Structures*, vol. 252, 2020.
[11] L. A. Piegl and W. Tiller. *The NURBS book*. Springer, 1997.
[12] J. Kennedy and R. Eberhart. *Particle swarm optimization*, volume 4. IEEE, 1995.
[13] D. Bratton and J. Kennedy. Defining a standard for particle swarm optimization. *2007 IEEE Swarm Intelligence Symposium*, vol. , 2007.
[14] E. S. Barroso, E. Parente, and A. M. C. Melo. A hybrid PSO-GA algorithm for optimization of laminated composites. *Structural and Multidisciplinary Optimization*, vol. 55, n. 6, pp. 2111–2130, 2017.
[15] A. C. C. Lemonge and H. J. C. Barbosa. An adaptive penalty scheme for genetic algorithms in structural optimization. *International Journal for Numerical Methods in Engineering*, vol. 59, n. 5, pp. 703–736, 2003.
[16] A. Sobester, S. J. Leary, and A. J. Keane. On the design of optimization strategies based on global response surface approximation models. *Journal of Global Optimization*, vol. 33, pp. 31–59, 2005.
[17] A. Mathern, O. S. Steinholtz, A. Sjöberg, M. Önnheim, K. Ek, R. Rempling, E. Gustavsson, and M. Jirstrand. Multi-objective constrained Bayesian optimization for structural design. *Structural and Multidisciplinary Optimization*, vol. 63, n. 2009, 2020.